DOI: 10.13009/EUCASS2023-876
Aerospace Europe Conference 2023 – 10TH EUCASS – 9TH CEAS

Design, Fabrication and Performance of Planar Solid Propellant Micro-thruster Based on SU-8 Photoresist

Jianbing Xu [1,2,3]†, Zehua Zhang [1,2,3], Fuwei Li [1,2,3], Jian Cheng [1,2,3], Yinghua Ye [1,2,3]†, Ruiqi Shen [1,2,3]
[1] *Department of Applied Chemistry, School of Chemistry and Chemical Engineering, Nanjing University of Science and Technology, Nanjing 210094, China*
[2] *Micro-Nano Energetic Devices Key Laboratory of MIIT, Nanjing 210094, China*
[3] *Institute of Space Propulsion, Nanjing University of Science and Technology, Nanjing 210094, China*
† Corresponding Author: xujianbing@njust.edu.cn & yyinghua@njust.edu.cn

Abstract
In order to meet the demand of small satellites for micro propulsion system, a Planar Solid Propellant Micro-thruster (PSPMt) was designed and fabricated. Using SU-8 photoresist as chamber material, a miniature combustion chamber with laval nozzle was fabricated with lithography technology. And the effects of coating, soft-bake, exposure and developing parameter on lithography result was also studied. The PSPMt was sealed with MD130 glue and its propulsive performance was tested by a micro-impulse testing platform. The impulse of the prepared PSPMt reaches 127.9 μN·s and its ignition duration lasts 0.2 ms when loaded with 1.9 mg nanothermite.

1. Introduction

Since the 1990s, space science and micro-electro-mechanical technology (MEMS) have developed rapidly. Compared to traditional satellites, with its incomparable advantages such as high functional density, rapid emergency response, low manufacturing cost, short research and development cycle, good stealth performance and low launch cost, micro-nano satellite has attracted extensive attention from many research teams and space departments of various countries[1-3]. With the development and application of micro-nano satellite technology, more and more urgent needs are put forward for micro-propulsion system. Due to the small size and mass of the micro-nano satellite and the small inertia of light rotation, it is necessary to develop a micro-propulsion system with high integration, low power consumption , small thrust (μN~mN) and micro impulse (10^{-9}~10^{-3} N·s), which suitable for orbit maintaining and attitude control of the micro-nano satellite [4,5]. At present, the main forms of micro-propulsion system include liquid evaporation, plasma air type and solid chemical type, etc. Among them, a class of solid chemical micro-thrusters based on MEMS technology has the advantages of simple structure, compact package, fast response, adjustable thrust and easy integration with other electronic devices, which is fully able to meet all kinds of demanding requirements proposed by the development of micro-nano satellite. It stands out from numerous micro-propulsion systems and has become a research hotspot in the field of micro-propulsion [6].
A typical solid chemical micro-thruster structure is mainly composed of an ignition circuit layer, a combustion chamber layer and a sealing layer [7], which is similar to a sandwich. The nozzle orientation of the planar micro-thruster is parallel to the base surface. With the help of MEMS technology, the nozzle shape and combustion chamber size can be designed according to the required thrust category. And due to the integrated design of the nozzle layer and combustion chamber, the alignment and bonding of the two can be eliminated, further reducing the technological process. SU-8 photoresist is a kind of negative, epoxy-type, near-ultraviolet photoresist. Its light absorption is very low in the range of near ultraviolet light (365nm-400nm), and the exposure of the whole photoresist layer is uniform and consistent, which can obtain thick film graphics with vertical side walls and high aspect ratio and form complicated structures such as steps. In addition, SU-8 photoresist forms a three-dimensional cross-linked structure owing to its cross-linking reaction after exposuring to ultraviolet light. It also has well mechanical properties, chemical corrosion resistance and thermal stability [9,10]. Thanks to these advantages, SU-8 photoresist is gradually applied in MEMS, chip packaging and micromachining fields. It is a novel technology in the field of micromachining to directly use SU-8 photoresist to produce microstructures and micro parts with high depth-width ratio [11]. In order to optimize the fabrication of combustor layer in planar solid chemical micro-thrusters, in this study, SU-8 photoresist was used to fabricate the combustor layer containing a small Laval nozzle, and the optimized parameters of combustion chamber

DOI: 10.13009/EUCASS2023-876

made by SU-8 photoresist were obtained. Finally, the sealing bonding of planar solid chemical micro-thruster was realized and its thrust performance was tested.

2. Design of PSPMt

2.1 Overall design of PSPMt

Planar solid chemical micro-thruster generally adopts a three-layer structure design, which consisted of three parts: ignition circuit layer， combustion chamber layer (charge chamber and Laval nozzle) and sealing layer, and its schematic diagram is shown in Figure 1. The bottom layer is the ignition circuit layer, and the metal film ignition bridge is deposited on the base. The two endpoints of the ignition bridge are led out of pad, which can be connected to an external logic control circuit module by leads. The middle layer is the combustion chamber layer, which integrates the charge chamber and Laval nozzle. The location of the ignition bridge is close to the Laval nozzle, which make the bridge contact with the propellant directly so that the bridge is able to ignite the propellant efficiently and reliably, thereby increasing the effective utilization rate of the agent, and the generated thrust (impulse) is also improved. The top layer is the sealing layer, which usually made by high-temperature resistant printed circuit board (PCB) as the main material. The MEMS low-temperature adhesive bonding process is used to make it bond with the combustion chamber layer, so that the heat generated in the process won't lost easily. The three-layer structure can be assembled into a whole by means of bonding. Its working principle is as follows: the temperature of the ignition bridge is continuously raised by constant current excitation, which heats the propellant in the chamber, and propellant burns producing a lot of gas which is accelerated through the throat of the nozzle and ejected outward to generate thrust when the heat accumulation reaches the ignition point of the propellant, by which the planar micro-thruster perform work externally. The manufacturing process of the whole micro-thruster is shown as follows:

(1) Fabricate ignition bridge, leads and pad on the substrate;
(2) Fabricate the combustion chamber layer integrated with the charge chamber and Laval nozzle;
(3) Bond the ignition circuit layer and the combustion chamber layer;
(4) Fill the propellant into the chamber;
(5) Bond the sealing layer.

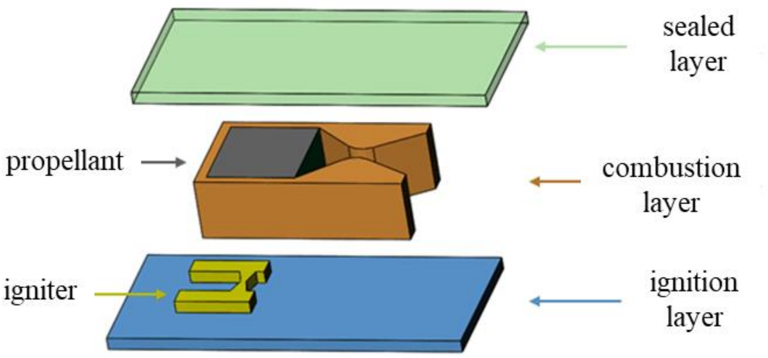

Figure 1: Schematic diagram of the PSPMt with "sandwich biscuit" structure

2.2 Design of PSPMt combustion chamber layer

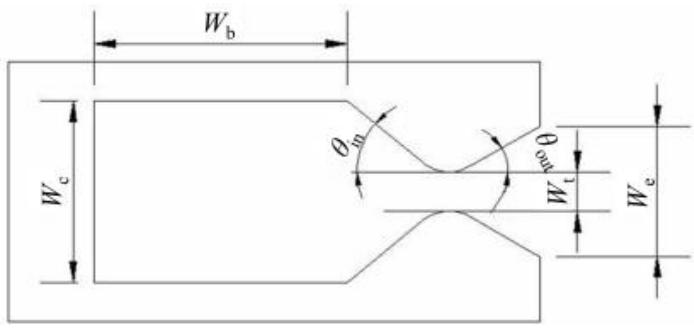

Figure 2: Plane sectional structure of the combustion chamber layer

DOI: 10.13009/EUCASS2023-876

The plane sectional structure of the combustion chamber is shown in Figure 2. Its geometric parameters include the following sections: width(W_c), length(W_b), radius of curvature of Laval nozzle throat(R_t), throat width(W_t), outlet width(W_e), convergence half angle(θ_{in}) and spread half angle(θ_{out}). According to the research results of preliminary simulation calculation in the laboratory [12], the combustion chamber layer of small Laval nozzle micro-thruster is designed as follows, the specific size parameters are shown in Table 1.

Table 1: Geometry parameter of Laval nozzle

W_c /mm	W_b /mm	R_t /mm	θ_{in} /°	θ_{out} /°	W_e /mm	W_t /mm
1.5	1.5	0.375	40	30	0.25	1.25

2.3 Design of PSPMt ignition layer

Due to the limited energy provided by the microsatellite, it is necessary to design an ignition bridge suitable for low current reliable ignition on the microsatellite. The Ni-Cr film ignition bridge was fabricated on ceramic substrate by MEMS process in preliminary study [13], which has good safety, rapid response and reliable ignition, therefore, the Ni-Cr film ignition bridge is selected in the micro-thruster. The production process is shown in Figure 3, 1.3μm Ni-Cr film was deposited on an Al_2O_3 ceramic substrate by magnetron sputtering firstly, after lithography, development, 1μm gold pad was electroplated, then the shape of ignition bridge was transferred to the substrate by lithography development and wet etching. At last, a single Ni-Cr film ignition bridge is obtained by laser scribing.

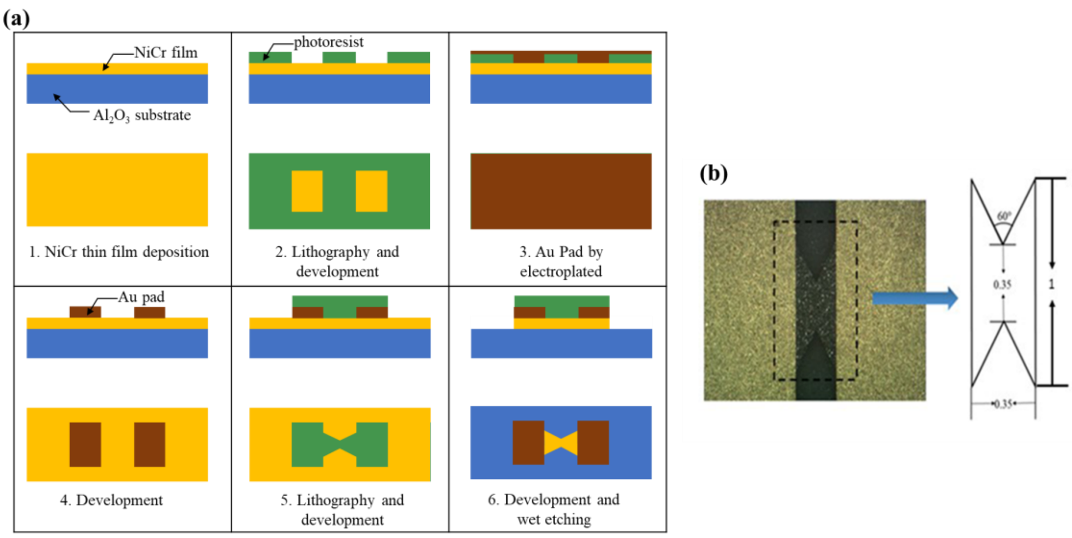

Figure 3: The fabrication process of Ni-Cr thin film ignition bridge and its actual image, (a) fabrication process, (b)sample of Ni-Cr thin film and bridge area size

2.4 Design of PSPMt sealing layer

The consideration for the material of the micro-thruster sealing layer is that it requires higher structural strength and lower thermal conductivity. In this study, PCB (main material is FR-4) was selected as the packaging material.

3. Fabrication and performance of PSPMt

3.1 The fabrication of a miniature combustion chamber with Laval nozzle

3.1.1 Setup and Materials

Setup: Programmed temperature control hot plate (type: HOTPLATE-100, manufacturer: Shanghai Kamet Functional Ceramics Technology Co., LTD), Spin coater (type: Spinmaster-100, manufacturer: Shanghai Kamet Functional Ceramics Technology Co., LTD), Confocal laser scanning microscope (type: Olympus Lext3100, manufacturer: Japan Olympus Co., LTD) and Ultraviolet (UV) lithography machine (type: URE-2000/35L, manufacturer: Institute

DOI: 10.13009/EUCASS2023-876

of Optoelectronics Technology, Chinese Academy of Sciences). The resolution of the UV lithography machine can reach 1.0μm, the parallelism of the light source is better than 1.5°, and the maximum focal thickness can reach 400μm. Materials: SU-8 photoresist 2000 series of SU-8 2150 photoresist (manufacturer: American Microlithography Chemical corporation), propylene glycol monomethyl ether acetate developer (manufacturer: Jiangyin Jianghua Microelectronic Materials Co., LTD), absolute alcohol (specification: analysis pure, purity content is greater than 99.7%, manufacturer: Sinopharm Chemical Reagent Co., LTD) and acetone (specification: analytical purity, purity content is greater than 99.5%, manufacturer: Shanghai Linfeng Chemical Reagent Co., LTD).

3.1.2 UV lithography process

The UV lithography process steps are as follows：

(1) Clean the substrate：First use ultrasound to immerse the substrate in an acetone solution for 15 min, then rinse with absolute ethanol for 15min in ultrasonic, and then rinse it repeatedly with deionized water, finally the cleaned substrate was blow-dried with hot nitrogen. Later it was placed in a vacuum oven with a temperature of 120^0C for 45 min, so as to remove the residual moisture on the surface and ensure that there is no oil stains, no dust and no moisture on the surface.

(2) Whirl coating: The thickness of the flat solid chemical micro-thruster combustion chamber shall be up to 400μm. In order to obtain a combustion chamber layer with benign evenness and suitable thickness, the process of whirl coating was used twice in the experiment while keeping the parameters of other steps unchanged. After medium drying, measure the thickness of the film so as to optimize the process parameters of the whirl coating, which shown in Table 2. Let substrate flow evenly in the air for half an hour to eliminate the surface tension between the SU-8 photoresist and the substrate after the whirl coating.

Table 2: The parameters of coating process

Experiment number	Step	Acceleration time /s	Number of revolutions / rpm	Holding time /s
Condition 1	First spin	5 8 7	500 1500 0	10 30 0
	Second spin	5 13 12	500 1800 0	10 30 0
Condition 2	First spin	5 8 7	700 1500 0	10 30 0
	Second spin	7 13 12	700 1800 0	10 30 0
Condition 3	First spin	7 8 7	700 1800 0	10 30 0
	Second spin	7 13 12	700 2000 0	10 30 0

(3) Soft bake: It is difficult to keep the same optical properties of the layers by two times of whirl coating and necessary to control the soft bake parameters of each layer accurately. A programmed temperature control hot plate is used to heat the coated base and heat is transferred upward from the bottom of the substrate, which is conducive to the evaporation of solvents in the photoresist, and the substrate is cooled to room temperature by the plate after each drying to ensure the surface smoothness of the film. The specific parameters of pre-drying process is shown in Table 3.

DOI: 10.13009/EUCASS2023-876

Table 3: The parameters of soft bake process

Test number	Step	Target temperature/ ℃	Rising (falling)temperature rate / ℃·min^{-1}	Holding time / min
Condition 1	First soft bake	65	10	10
		95	10	20
		25	10	30
	Second soft bake	65	10	10
		95	10	70
		25	10	30
Condition 2	First soft bake	65	10	10
		95	10	40
		25	10	30
	Second soft bake	65	10	10
		95	10	80
		25	10	30

(4) Exposure: The power of the UV lithography machine is 24mW, and different exposure parameters were set, namely 15s, 25s, 35s, 45s and 55s, to explore the influence of exposure time on the film forming quality.
(5) Medium bake: SU-8 photoresist was cross-linked by strong acid generated during exposure at high temperature. The parameters of medium drying process were shown in Table 4.

Table 4 The parameter of medium bake process

Target temperature/ ℃	Rising (falling) temperature rate / ℃·min^{-1}	Holding time / min
65	10	10
95	10	30
25	10	30

(6) Development was carried out after cooling the substrate to room temperature, and the development time was set as 15min, 30min, 45min and 60min respectively. After development, the substrate was removed from the developer, cleaned repeatedly with deionized water, and then dried with hot nitrogen.
The structure of Laval nozzle in the combustion chamber layer was observed and measured with a confocal laser microscope. Explore the influence of different process conditions on lithographic patterns so as to optimize the optimum photoresist parameters.

3.1.3 Discussion of experimental results

(1) The impact of coating
When dump the photoresist on the substrate, the film with different thickness and flatness can be obtained at different rotating speeds. In the three groups of experiments, the test results of the film thickness obtained were shown in Table 5. It can be seen that the thickness of the film is not the same under different conditions. Due to the slow speed, the thickness of film under condition 1 was the highest, but the smoothness was not good. The film thickness was thinner because of the faster speed under condition 3. The film under condition 2 was smooth and the desired thickness was achieved, therefore, condition 2 was determined as the best process condition.

Table 5: The film thickness under different coating parameters

Test number	Thinkness/μm					Average thickness/μm
1	470	490	430	442	480	462.4
2	380	370	383	400	400	382.6
3	290	290	340	310	310	308.0

(2) The impact of soft bake
Under the condition 2 and the same exposure condition, two different soft bake process parameters were set, as shown in Table 3. Soft bake tends to lead to uneven distribution of molecular concentration in the longitudinal direction of su-8 photoresist, and the concentration closest to the base is generally higher than the top. Other steps were controlled

DOI: 10.13009/EUCASS2023-876

to remain unchanged, and the figure of Laval pipe nozzle in the chamber obtained under two different soft bake conditions was shown in Figure 4. According to the forming conditions of Laval nozzle, there were obvious differences in optical properties of the film in Figure 4(a), and the upper layer was etched relatively clean, while the lower layer had more burrs. Lamination didn't occur in Figure 4(b), the reason was that the uneven distribution of solvents in the lower layer in Figure 4(a) resulted in the interfacial delamination of excessive cross-linking of the photoresist. Therefore, it was believed that keep 95° C for a longer time was conducive to the uniform distribution of the solvent in the first soft bake, which could make the photoresist distribute well in unit volume, moderate the proportion, increase the cross-linking degree of photoresist and improve the linear shape. If the time is too long, it will lead to the excessive cross-linking during the medium bake process, generate internal stress between the photoresist and substrate and make the substrate bend. In addition, the shorter soft bake time which caused the mask and the photoresist to stick together at the exposure time, also resulted in poor quality of the graphics produced later and contaminating the mask. Therefore, the soft bake parameter 2 is better than the pre-drying parameter 1.

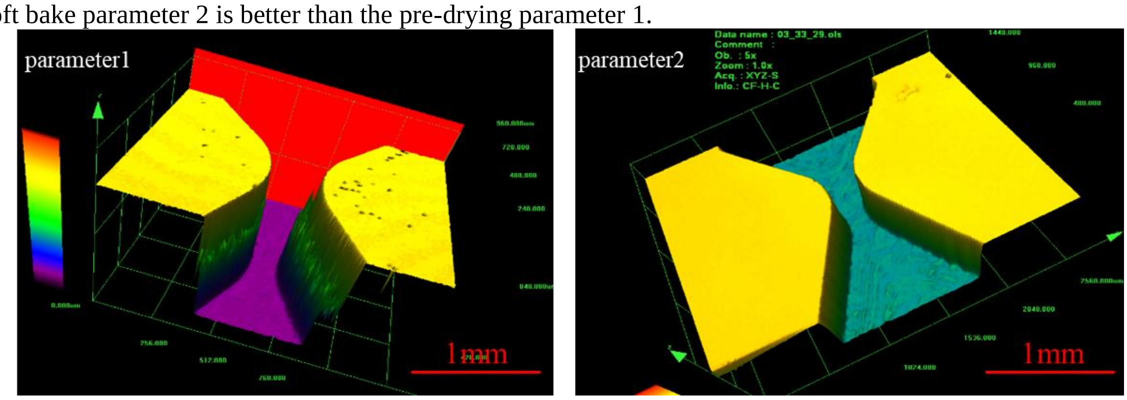

a. parameter 1 **b.** parameter 2

Figure 4: The nozzle image under different soft bake parameters

(3) The impact of exposure

The common exposure method includes contact exposure and non-contact exposure. Contact exposure refers to direct contact between the photo mask and the substrate coated with photoresist. Theoretically, the gap between the photoresist surface and the photo mask is zero, thus, diffraction does not occur during exposure, and the resolution of the image produced by it is higher than that of non-contact exposure. URE-2000/35L UV lithography machine is vacuum contact exposure, therefore, the influence of the gap between the photoresist surface and the mask and the air on the exposure process was ignored, and the coupling effect of the reflected light and the incident light generated at the contact interface between the photoresist and the substrate was not considered. The exposure dose is the product of the light intensity and the exposure time, and the light intensity is mainly affected by the wavelength of the light. The experiment used the UV-365nm band light source, so the influence of the exposure time on the final shape of the graph was mainly discussed.

In this paper, the line-width deviation and inclination angle of the device manufactured at different exposure times were measured respectively. The measurement results were shown in Figure5,where the line-width deviation refered to the difference between the size of the made graph and the designed. Inclination refers to the angle between the formed side wall and the horizontal direction, as shown in Figure 6.The experimental results showed that, within a certain range, with the increase of exposure time, the line-width deviation decreased gradually until it reached the minimum value. When the exposure time increased to exceed the optimal exposure time, the line-width deviation increased and finally tended to be stable. The change of inclination also showed the same law, within a certain range, with the increase of exposure time, the inclination gradually increases until it reached the maximum value. When the exposure time increased to exceed the optimal exposure time, the inclination decreased and finally tended to be stable. The reason for the above phenomenon might be that there were few molecules involved in crosslinking and the polymer chain formed was not tight enough, resulting in swelling phenomenon and then a larger line width. When the exposure time was moderately increased, the number of molecules involved in cross-linking increased, forming a dense polymer chain, swelling phenomenon would be alleviated, thus reducing the line width. But once the optimal exposure time was exceeded, too many molecules participated in the crosslinking, and the line width increased again. From the analysis of experimental results, the best exposure time was 25s.

DOI: 10.13009/EUCASS2023-876

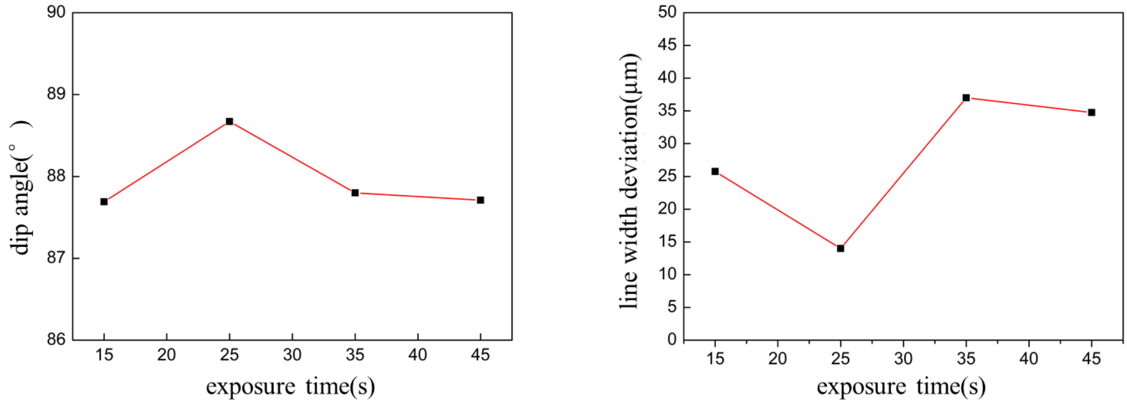

a. dip angle **b.** line width deviation

Figure 5: Variation curve of line width deviation and dip angle at different exposure time

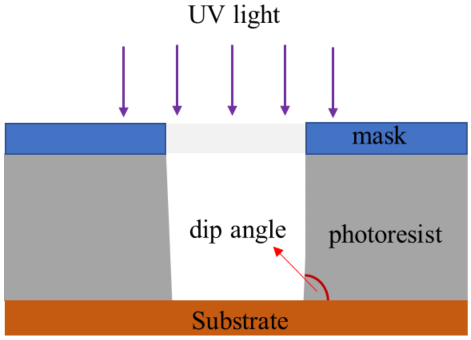

Figure 6: Schematic diagram of the dip angle in of lithographic process

(4) The impact of development time

After the medium bake, the cooled substrate was placed in the developer which could dissolve the unexposed part. Magnetic stirrer was used to stir the developer and make it penetrate into the photoresist so as to speed up the development process. In the case of underexposure, the variation of inclination angle and line width deviation was shown in Figure 7. The main reason was that the degree of cross-linking was small and the network structure formed was not compact enough, resulting in a large swelling phenomenon. However, the swelling phenomenon also has a certain limit, when the development time reaches a certain value, it tends to saturation. When the exposure parameter was optimal, the variation of inclination angle and line width deviation was shown in Figure 8. The main reason might be that the solvent was not uniformly distributed in the longitudinal direction during the pre-drying process, that is, the concentration distribution of the photoresist was not uniform. In addition, the SU-8 photoresist which close to the mask surface could receive more light intensity, so the top molecule cross-linking is relatively tight, and the bottom layer is relatively loose. According to the analysis of the results, the effect was better when the development time was 30mins. If the development time is longer, the figure is easy to fall off from the base.

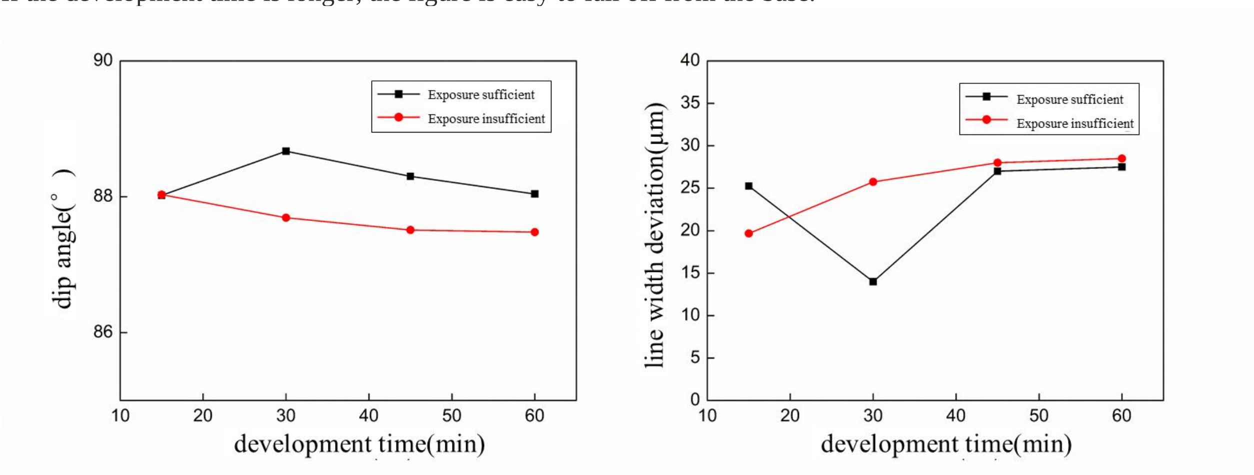

a. dip angle **b.** line width deviation

Figure 7: Variation curves of line width deviation and dip angle with development time under different conditions

DOI: 10.13009/EUCASS2023-876

Based on the above description, the optimum parameters of SU-8 photoresist lithography process were shown in Table 6 and 7, the optimum exposure time was 25s, and the optimum development time was 30min. The structure of the planar solid chemical micro-thruster was shown in Figure 8.

Table 6: The optimum coating process parameters

Step	Acceleration time /s	Revolution / rpm	Holding time /s
The first coating	7	700	10
	8	1500	30
	7	0	0
The second coating	7	700	10
	13	1800	30
	12	0	0

Table 7: The optimum bake process parameters

step		Target temperature/ ℃	Rising (falling) temperature rate / $℃\cdot min^{-1}$	Holding time / min
Soft-bake	The first soft-bake	65	10	10
		95	10	40
		25	10	30
	The second soft-bake	65	10	10
		95	10	80
		25	10	30
Medium bake		65	10	10
		95	10	30
		25	10	30

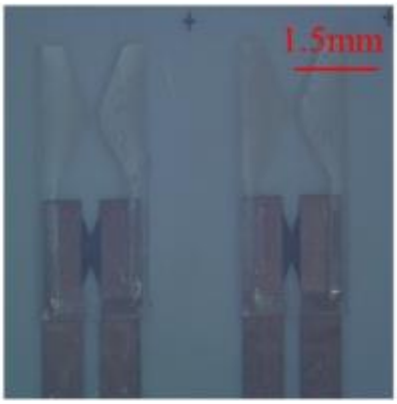

Figure 8: The fabricated combustion chamber structure of PSPMt

3.2 Low temperature bonding of PSPMt

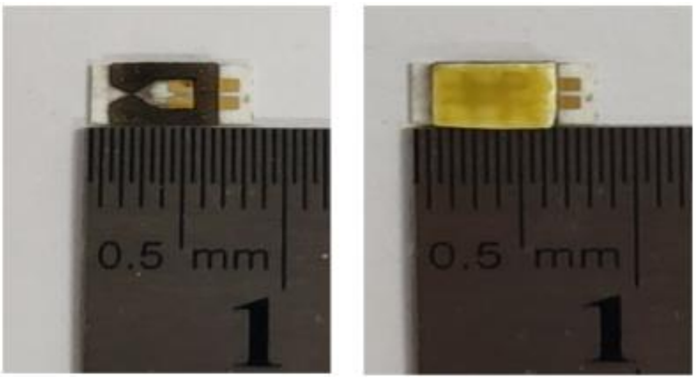

before bonding after bonding

Figure 9: The PSPMt fabricated with SU-8 photoresist bonded by MD130 adhesive

DOI: 10.13009/EUCASS2023-876

The charge volume and quantity of planar micro-thruster is small. In order to improve the safety and charge consistency of the charging process, nano aluminum and copper oxide particles (homemade by NJUST) and nitrocotton was added into solvent DMF(N, N-dimethyl formamide) to prepare energy-containing ink. Use the three-dimensional rapid prototyping platform to fill the energy-containing ink into the micro-thruster chamber [14] and realize the in-situ charge of the energy-containing ink. Weigh the mass of the micro-thruster before and after charging and calculate the charge mass. The micro-thruster shall be loaded with 1.9mg energy-containing ink. MD130 space adhesive was used as adhesive for micro-thruster. The low temperature bonding technology was used to complete the bonding of the ignition circuit layer, the combustion chamber layer and the sealing layer. The actual bonding of the ignition circuit layer and the combustion chamber layer made of Su-8 photoresist was shown in Figure 9.

3.3 The thrust performance test of PSPMt

Thrust (impulse) is a key parameter of the micro-thruster. In this paper, a self-designed torsion pendulum structure testing device was selected [15]. The testing device is consisted of the following five parts: torsion balance, displacement sensor, electromagnetic damper, counterweight and calibration system. The measurement error caused by damping is less than 10^{-4} and can be ignored. The maximum torsion pendulum displacement of the testing device is less than 6mm. Through calculation, it could be known that its impulse range is $4.1*10^{-7}$ N·s~5.4 $*10^{-3}$ N ·s, which could meet the precise measurement of nN~mN magnitude thrust. The schematic diagram of the test device was shown in Figure 10.

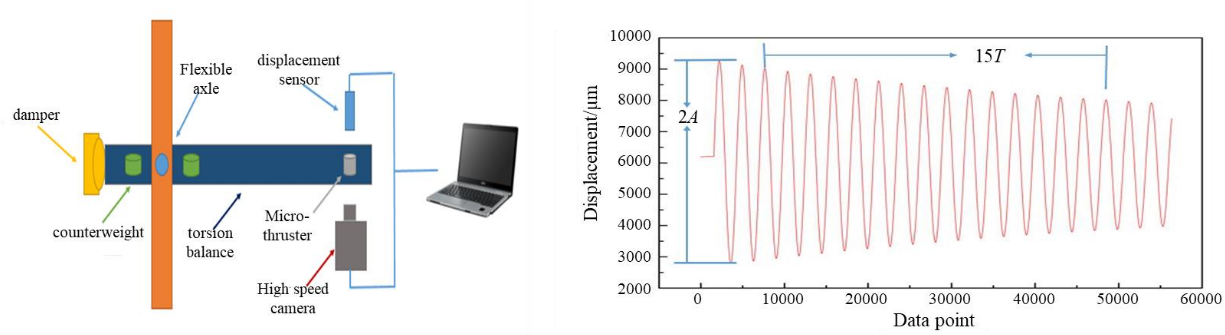

micro impulse testing setup typical displacement curve

Figure 10: Diagram of micro impulse testing stand and typical testing displacement curve

The device is mainly consisted of a planar micro-thruster, a high-speed camera (model: MotionXtra HG-100K, manufacturer: Redlake Co.,LTD), a laser displacement sensor (model: CCS-100-N3, manufacturer: French STIL), and a customized constant current stabilized voltage source. High-speed photography records the combustion of propellant synchronously with a sampling frame rate of 10000fps. The constant current stabilized voltage source provides the required ignition current to the ignition bridge. The gas produced by combustion is ejected to produce thrust and the swinging displacement of the system is collected by the laser displacement sensor. The torsion pendulum displacement curve of a typical micro-impulse test is shown in Figure 11. The abscissa of the curve is the data point collected by the laser displacement sensor, the ordinate is the torsion pendulum displacement, and the maximum displacement A is the difference between the first crest and the baseline. According to the calibration, the relationship between the maximum torsion pendulum displacement A (μm), period T (s) and impulse I (N·s) was determined as follows:

$$I=1.805*A/T \tag{1}$$

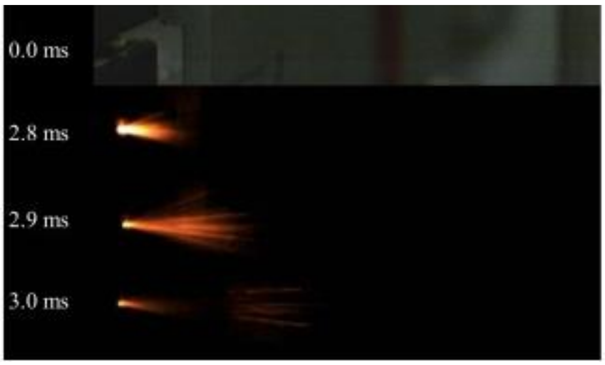

Figure 11: The ignition process of the PSPMt

DOI: 10.13009/EUCASS2023-876

The impulse test result of the micro-thruster made of SU-8 photoresist is 127.9 μN·s. The ignition and combustion process of propellant was shown in Figure 11, and it could be seen that the ignition delay time is 2.8 ms. In the initial stage of ignition, the propellant combustion produced high temperature and pressure gas, which was accelerated through Laval nozzle together with the high heat combustion products and ejected from the nozzle on the side. As more propellant was ignited, the combustion tail flame growed further, became less bright, and gradually died out. The entire combustion process lasted for 0.2 ms.

4. Conclusion

Use SU-8 photoresist as chamber material, and the lithography process was used to fabricate the layer of combustion chamber with Laval nozzle, and the appropriate lithography parameters were studied: The sealing bonding of planar solid chemical micro-thruster was realized with MD130 glue, and its propulsive performance was tested by micro-impulse test platform. The main conclusions were as follows:
(1) The speed of coating determines the thickness of the film. The faster the speed, the thinner the film. When the coating parameter is condition 2, it is beneficial to obtain a film with good flatness which thickness is close to 400 μm.
(2) The soft bake has a great influence on the properties of the film. Properly increase the soft bake time can reduce the interface difference of the second coating and distribute the photoresist more evenly. If the time is too long, it will cause excessive cross-linking during the medium baking. Make the photoresist and the substrate generate internal stress to cause the substrate bend, so the soft bake parameter 2 is better than the parameter 1.
(3) Insufficient and excessive exposure time both will make the line width deviation larger. After the exposure time exceeds a certain time, the line width deviation will remain unchanged. Proper exposure time is conducive to reducing the line width deviation. The best exposure time is 25 s.
(4) In the case of underexposure, the development process will cause swelling, which makes the line width deviation larger. The development effect is well when the development time is 30 min. If the time is longer, the graphics will easily fall off the substrate.
(5) The micro-thruster made of SU-8 photoresist was loaded with 1.9 mg of nano-thermite, and the micro-impulse test platform was used to obtain an impulse of 127.9 μN·s under the excitation of a pulse current of 5A3ms, and the ignition duration was 0.2 ms.

References

[1] Rycroft M J, Crosby N. Smaller satellites: bigger business?: Concepts, Applications and Markets for Micro/Nanosatellites in a New Information World[M]. Springer Science & Business Media, 2013.
[2] ZHU Zhen-cai, ZHANG Ke-ke, CHEN Hong-yu, et al. Microsatellite design and engineering practice[M]. Beijing: Sciene Press, 2016.
[3] Janson S W, Helvatian H, Hansen W W, et al. Microthrusters for nanosatellites[C] The Second International Conference on Integrated Micro Nanotechnology for Space Applications (MNT99). Pasadena, CA, 1999.
[4] YOU Zheng, ZHANG Gao-fei. An review of MEMS-based micropropulsion developments[J]. *Microfabrication Technology*, 2004, (01): 2-9.
[5] RU Cheng-bo, XU Jian-bing, Dai-Ji, et al. A summary of MEMS based solid propellant microthrusters (SPM) Array[J]. *Explosive Materials*, 2016, 45(06): 4-13.
[6] ZHANG Bo-bin, YANG Yi-ting. Research progress of solid propellant micropropulsion system based on MEMS[J]. *Aerospace China*, 2018, 484(08): 65-69.
[7] Lewis D H, Janson S W, Cohen R B, et al. Digital micropropulsion[J]. *Sensors and Actuators A: Physical*, 2000, 80(2): 143-154.
[8] Rossi C, Briand D, Dumonteuil M, et al. Matrix of 10×10 addressed solid propellant microthrusters: review of the technologies[J]. *Sensors and Actuators A: Physical*, 2006, 126(1): 241-252.
[9] ZHANG Zhi-zhong, WANG Bo-zhou, ZHU Chun-hua, et al. Study on sythesis of ADN(II)[J]. *Chinese Journal of Energetic Materials(Hanneng Cailiao)*, 2001, 9(3): 97-99.
[10] CHUNG S, PARK S. Effects of temperature on mechanical properties of SU-8 photoresist material[J]. Journal of Mechanical Science and Technology, 2013, 27(9): 2701-2707.
[11] LIU Jian-zhong, LIANG Dao-lun, WANG Yang, et al. Review on MEMS-Based solid propellant micro-propulsion. *Nanotechnology and Precision Engineering*, 2016, 14(1): 52-58.
[12] WANG Fei. Structural design and propellant performance of a horizontal micro-thruster[D]. Nanjing: Nanjing University of Science and Technology, 2018.
[13] YANG Teng-long, SHEN Yun, Dai Ji, et al. Fabrication and Characterization of a Ni-Cr@Al/CuO Insensitive Energetic Element. *Chinese Journal of Energetic Materials(Hanneng Cailiao)*, 2019, 27(10):830-836.

DOI: 10.13009/EUCASS2023-876

[14] XING Zong-ren. Research of three-dimensional printing for energetic materials[D]. Nanjing: Nanjing University of Science and Technology, 2012.
[15] WANG Xiao-yong. Study on the technology of laser ablation micro-propulsion based on the GAP[D]. Nanjing: Nanjing University of Science and Technology, 2015.